ASME Journal of Biomechanical Engineering
Online journal at:
https://asmedigitalcollection.asme.org/biomechanical

Joy A. Iaconianni
Drexel University,
3120 Market Street, Bossone 713,
Philadelphia, PA 19104
e-mail: jai37@drexel.edu

Sriram Balasubramanian
School of Biomedical Engineering,
Drexel University,
3120 Market Street, Bossone 713,
Philadelphia, PA 19104
e-mail: sri.bala@drexel.edu

Michele J. Grimm
College of Nanotechnology, Science, and Engineering,
University at Albany,
1400 Washington Ave,
Albany, NY 12222
e-mail: mgrimm@albany.edu

Bernard Gonik
Obstetrics & Gynecology — School of Medicine,
Wayne State University,
3990 John R. Street, 7 Brush North,
Detroit, MI 48201
e-mail: bgonik@wayne.edu

Anita Singh[1]
Mem. ASME
College of Engineering,
Temple University,
Engineering Building Room 601,
Bioengineering, 1947 N. 12th Street,
Philadelphia, PA 19104
e-mail: anita.singh0001@temple.edu

Studying the Effects of Shoulder Dystocia and Neonate-Focused Delivery Maneuvers on Brachial Plexus Strain: A Computational Study

The purpose of this computational study was to investigate the effects of neonate-focused clinical delivery maneuvers on brachial plexus (BP) during shoulder dystocia. During shoulder dystocia, the anterior shoulder of the neonate is obstructed behind the symphysis pubis of the maternal pelvis, postdelivery of the neonate's head. This is managed by a series of clinical delivery maneuvers. The goal of this study was to simulate these delivery maneuvers and study their effects on neonatal BP strain. Using MADYMO *models of a maternal pelvis and a 90th-percentile neonate, various delivery maneuvers and positions were simulated including the lithotomy position alone of the maternal pelvis, delivery with the application of various suprapubic pressures (SPPs), neonate in an oblique position, and during posterior arm delivery maneuver. The resulting BP strain (%) along with the required maternal delivery force was reported in these independently simulated scenarios. The lithotomy position alone served as the baseline. Each of the successive maneuvers reported a decrease in the required delivery force and resulting neonatal BP strain. As the applied SPP force increased (three scenarios simulated), the required maternal delivery force and neonatal BP strain decreased. A further decrease in both delivery force and neonatal BP strain was observed in the oblique position, with the lowest delivery force and neonatal BP strain reported during the posterior arm delivery maneuver. Data obtained from the improved computational models in this study enhance our understanding of the effects of clinical maneuvers on neonatal BP strain during complicated birthing scenarios such as shoulder dystocia.* [DOI: 10.1115/1.4064313]

Introduction

Shoulder dystocia is the obstruction between the anterior shoulder of the neonate and the symphysis pubis of the maternal pelvis [1–3]. It is an unpredictable event and is classified as an obstetric emergency in which both the mother and neonate are at risk of injury. Shoulder dystocia has a prevalence rate of 0.2 to 3% during vaginal deliveries and is associated with risk factors such as fetal macrosomia, multiparous mothers, prolonged labor, maternal gestational diabetes, and high maternal body mass index (BMI) or weight-to-height ratio [2,4,5]. Having one or more of the listed factors can increase the risk of shoulder dystocia occurrence, although with a low predictive value. Shoulder dystocia can lead to overstretching of the brachial plexus (BP) causing neonatal brachial plexus palsy (NBPP) [6–8], and occurs in every 1.5 in 1000 births. While NBPP spontaneously recovers in 70–75% of cases; 25–30% of cases report no recovery and are diagnosed as Erb's or Klumpke's palsy, which is permanent paralysis of various muscles of the affected arm [5,8–11].

During complicated delivery scenarios, when shoulder dystocia is diagnosed, clinicians have a very limited amount of time to alleviate the obstruction before a severe injury to the infant or mother can occur. Clinicians perform maneuvers sequentially, increasing in difficulty and invasiveness, to achieve successful delivery. The lithotomy position (treated as the baseline in this study) is typically the starting birthing position where the mother is supine on the delivery table with legs flexed and feet separated and elevated in stirrups. When shoulder dystocia is diagnosed, a clinician first places the mother in McRoberts' position, with the thighs flexed and abducted to rotate the pelvis and flatten the sacrum. They then apply suprapubic pressures (SPP), in which forces are applied to the soft tissue superior to the maternal symphysis pubis to adduct the neonatal shoulders or rotate the shoulder away from the symphysis pubis and alleviate the obstruction [12]. If shoulder dystocia persists, rotational maneuvers are then performed, such as the Wood's Screw or Rubin's maneuver. This approach allows the bisacromial

[1]Corresponding author.

Manuscript received May 6, 2023; final manuscript received November 2, 2023; published online January 3, 2024. Assoc. Editor: Spencer P Lake.

diameter (i.e., width of the shoulder) to utilize the oblique diameter (i.e., largest width) of the gynecoid pelvis [3,13,14]. If delivery remains unsuccessful, posterior arm delivery is then attempted—in which the clinician reaches inside the birth canal to adduct and bring the posterior arm across the infant's chest and out past the neonate's head, delivering the posterior arm of the neonate before the shoulders. This effectively reduces the shoulder width, thereby alleviating the obstruction and resulting in the delivery of the neonate [15].

Previous studies investigating these maneuvers have reported a high delivery success rate for the McRoberts maneuver when performed with the application of SPP [16,17]. Another case study reported oblique or posterior arm delivery maneuvers to be more effective (in 74% of vaginal births) than McRoberts and SPP [18]. Furthermore, Leung et al. reported a reduction in BP strain with rotational or oblique maneuvers [19]. While these studies offer some insight into the effects of delivery maneuvers during complicated birthing scenarios, additional studies are needed to further enhance our understanding of the effects of these clinical maneuvers on neonatal BP strain that leads to the observed NBPP injuries.

Ethical and technical limitations in performing investigational clinical studies to better understand injuries sustained during birthing complications increase reliance on surrogates such as computational models [14]. These models can be used to study the effects of various delivery maneuvers that are used to manage shoulder dystocia and the biomechanical response of neonatal BP in these complicated birthing scenarios [20]. While previous MADYMO modeling studies have laid a foundation for such an approach, those models have several limitations, including the model parameters that were not representative of neonatal BP tissue, as well as the limited simulations performed. The current study aims to fill these research gaps by enhancing the biofidelity of existing MADYMO models and further investigating the effects of shoulder dystocia and clinically applied neonate-focused delivery maneuvers on neonatal BP strain.

Materials and Methods

Mathematical Dynamic Models/MADYMO (v2020.2, Siemens Inc., OR) is a computational modeling software package that combines multibody systems and finite element modeling. Its most common application is automotive crash safety testing, where parameters such as position, force, velocity, acceleration, and coefficients of friction can be inputs and outputs of the performed simulations. In this study, MADYMO was utilized to develop models of the neonate and maternal pelvis, which were then used to simulate shoulder dystocia and various clinical delivery maneuvers. The neonate and maternal pelvis MADYMO model parameters including size, mass, joints, contact surfaces, force vectors, and position in the reference space to represent vaginal delivery were carefully defined from available literature [21,22]. The force required for delivery and relative elongation of the BP nerve (BP strain %) were recorded from the MADYMO output file while simulating various clinical maneuvers commonly utilized during complicated shoulder dystocia delivery.

The neonate and maternal pelvis MADYMO models used for the application of shoulder dystocia were originally developed by Zhang et al. in 2003 [23], using version 5.4 of the software. For this project, version 2020.2 of MADYMO was used, and all model components were updated. The neonate model developed by Zhang et al. (by scaling down the 9-month-old anthropomorphic test dummy model obtained from the MADYMO dummy database) was revised such that the new neonate model's weight (3.8 kg), height (53 cm), shoulder breadth (14 cm), chest breadth (12 cm), head circumference (36 cm), and chest circumference (35 cm) matched the measurements reported by the Center for Disease Control (CDC) [24]. The neonate model consisted of 32 ellipsoidal bodies that were connected by kinematic joints, and the BP was modeled as a bi-linear spring using the "belt" function in MADYMO. This function outputs force and length measurements that act on the belt throughout the simulation. The belt was defined by its original length of 7.5 cm, two points of attachment (below the C5 vertebra and at the midpoint of the upper arm), and stiffness. The maternal pelvis was created as a separate multibody system using a computer-aided design based on a computed tomography scan of a 50th-percentile female gynecoid pelvis and had an obstetric conjugate of 12.5 cm [23].

Previously developed MADYMO models were carefully reviewed when developing the MADYMO neonate and maternal pelvis models in the current study. The previously developed neonate MADYMO model reported a 90th-percentile neonate with a bisacromial diameter of 14.2 cm. The bisacromial diameter is the largest width of the neonatal shoulder and is measured between the outer shoulders [13]. The 90th percentile neonatal model was elected to offer a distinct size discrepancy between the neonatal shoulders and maternal pelvic inlet. This size discrepancy helped achieve the obstruction between the neonatal and maternal pelvic models simulating complicated shoulder dystocia scenarios. Figure 1 shows the neonate and maternal pelvis models at the start of the simulations. It is noteworthy that the acquired neonatal model, from the previously reported study [12], measured a bisacromial diameter of 12.4 cm, which is similar to that of a 50th-percentile neonate [23]. In this study, the neonate model was developed with a bisacromial diameter of 14.0 cm, which is reported for a 90th-percentile neonate [25]. This was achieved by scaling the neonate model by a factor of 1.13 such that the head-to-shoulder and head-to-body ratios were maintained.

The previously developed neonatal MADYMO model also reported that the origin of the neonate BP was between the C5 and C6 vertebrae; however, the acquired model had the BP originating between the C4 and C5 vertebrae [23,26]. In the current neonate model, the origin of the BP was between the C5 and C6 vertebrae and thus replicated the anatomical accuracy [27].

The MADYMO interface requires force–displacement values as inputs in the loading function to characterize the elastic properties of the modeled BP. The neonatal BP in the previously reported model included stress–strain data obtained from the rabbit tibial nerve published by Rydevik et al. (1990) [28]. In the current study, we improved the biofidelity of the neonate model by utilizing the force–displacement values from the musculocutaneous (MSC) nerve of neonatal piglets when subjected to tensile failure in vitro, as published by Singh et al. [20]. The MSC BP force–displacement values were scaled to be applied to the 7.5 cm long BP in the current

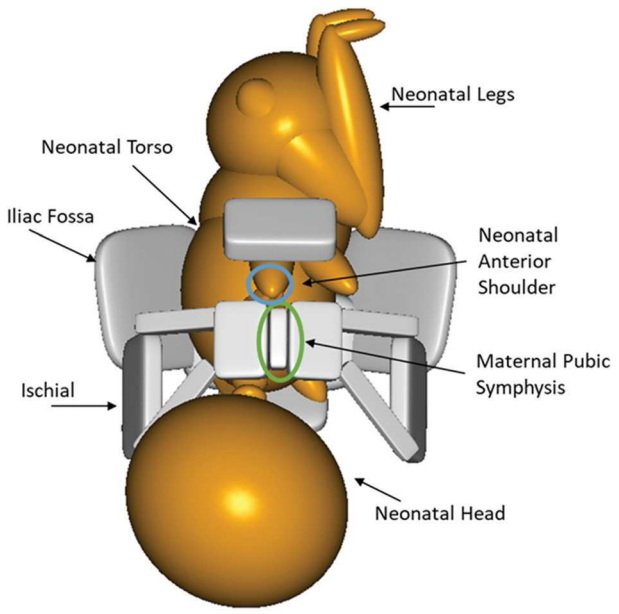

Fig. 1 The neonate (orange) and maternal pelvis (light grey) models in MADYMO at the start of the simulation in the lithotomy position

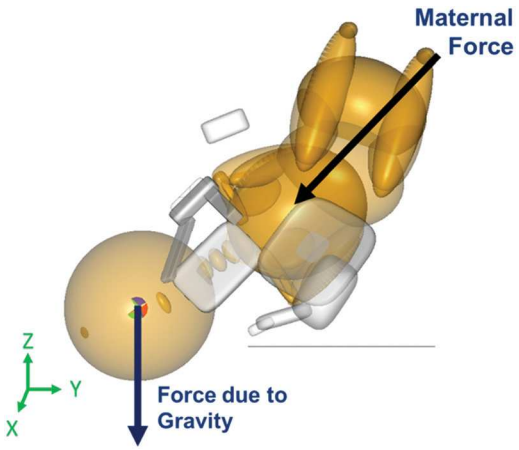

Fig. 2 Force vector for gravity applied to the center of gravity of the neonate's head and maternal force applied in line with the neonatal spinal axis in the current MADYMO models

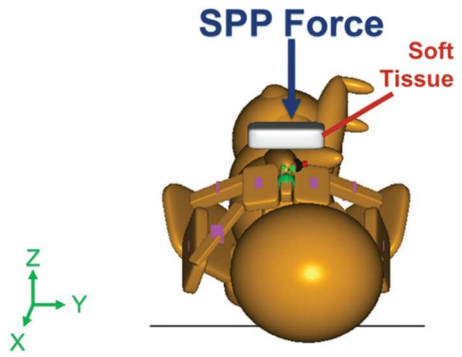

Fig. 4 Force vector of suprapubic pressure applied by the clinician at magnitudes of 40N, 80N, or 140N

model [26]. The BP was modeled as a one-dimensional bi-linear spring (using "belt" MADYMO function) with force–displacement values from the piglet nerve data to create a bi-linear load versus displacement curve with two linear sections. The stiffness values assigned to the first linear section was 227.65 N/m and the second linear section was 251.81 N/m which were obtained from in vitro BP tensile test [20].

Furthermore, unlike the previously developed models that applied gravity using a function that applied an acceleration field to the entire system [23], the current study utilized a body actuator function in MADYMO, which better replicates the delivery simulations. This function specifies the magnitude and direction of the gravitational force with respect to the reference space. In the current study, gravity was applied at the center of gravity of the neonate's head in the downward *Z*-direction, as shown in Fig. 1.

In addition to gravity, the neonate model in the current study was also subjected to published maternal forces that simulated combined maternal uterine contractions and Valsalva forces [14]. The maternal force was applied to the center of gravity of the neonate's upper torso using the body actuator function, as described previously. The previous MADYMO model applied maternal force at the center of mass of the neonate's torso at an angle of 25 deg below the horizontal—aligned with the angle of the infant's body [23,26,29,30]. In the current model, the expulsive maternal force was applied downward and outwards with respect to the birth canal at a 45 deg angle to follow along the axis of the neonate's spine [26], thereby resulting in a force direction between the negative *Z* and negative *Y* axes (Fig. 2). Contact characteristics between the surfaces of the maternal pelvis and neonate models were added and defined in the current models so that the systems would not penetrate each other when subjected to applied forces. This was achieved in the MADYMO software by defining rigid bodies as master and slave surfaces which were then assigned loading functions to define low elasticity and penetration of the rigid structures. The elastic load values were determined by evaluating the simulations and increasing the load until no penetration between the rigid bodies was observed. Rigid structures of the maternal pelvis and neonate were assigned friction coefficients of 0.2 and 0.6, respectively, as defined in the original models [23,26].

All delivery scenarios for this study involved maintaining the orientation of the maternal pelvis based on a lithotomy position—with the angle between the symphysis pubis and the horizontal (*X*–*Y*) plane being set at 45 deg. The initial position of the neonate model was such that the anterior shoulder was in contact with the symphysis pubis of the maternal pelvis, with the neonate head already delivered shown in Fig. 3. The models were oriented such that the midcoronal plane of the neonate was coplanar with the midsagittal plane of the maternal pelvis, shown in Fig. 3.

To simulate the application of SPP force, a body actuator was applied to a rigid body that was modeled to represent soft tissue superior to the maternal symphysis pubis bone. A body actuator is a MADYMO function that applies a concentrated load on a defined body with a defined magnitude and direction [31]. Since MADYMO is limited to rigid structures, soft tissue could not be accurately modeled. However, the rigid structure was modeled with a penetrative surface. The soft tissue of the mother was used to transfer the force applied by the clinician to the neonatal shoulder. The force was applied directly downwards in the Z-direction at 40N, 80N, or 140N, as shown in Fig. 4. The vector showing SPP force indicates the body actuator that was simulated at three levels. The next maneuver modeled was the oblique positioning of the neonate, shown in Fig. 5. In previously published studies, the neonate model was rotated by 15 deg in the counterclockwise direction anteriorly with respect to the midsagittal plane of the maternal pelvis model [23,26]. The current neonate model was rotated 30 deg clockwise (posteriorly) with respect to the midsagittal plane of the maternal

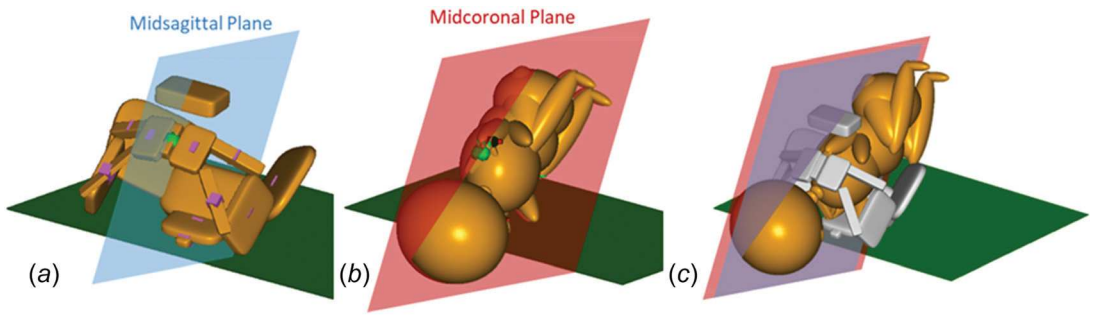

Fig. 3 Maternal pelvis model (*a*) and neonate model (*b*) in MADYMO and the initial position for lithotomy (*c*) with the midsagittal plane of the pelvis and midcoronal plane of the neonate coplanar relative to each other

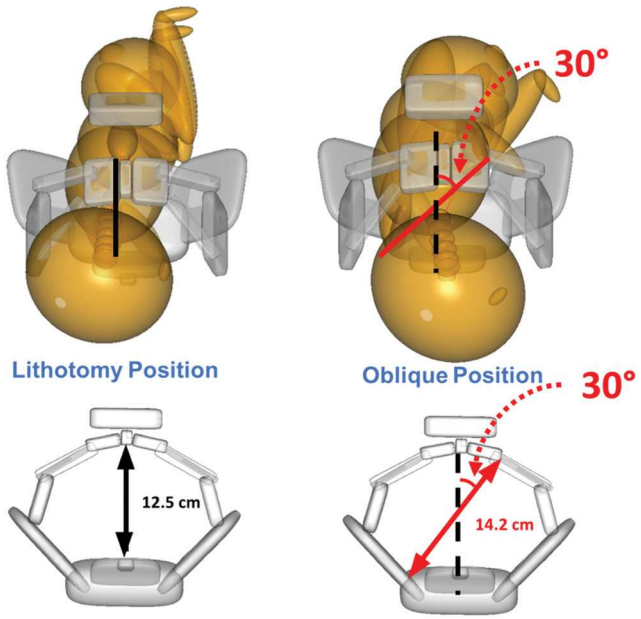

Fig. 5 Lithotomy (baseline) position (top left) compared to the oblique position (top right) of the neonate model and measurements of pelvic diameters in these positions (bottom)

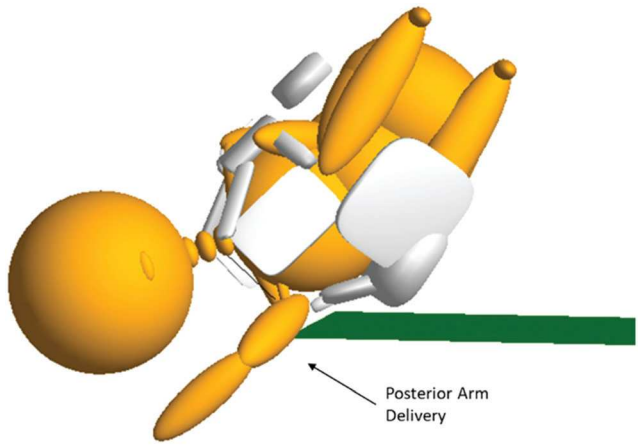

Fig. 6 Posterior arm delivery maneuver model in which the posterior arm was delivered prior to the anterior shoulder of the neonate

pelvis as widely reported in the literature. Common clinical practice includes rotational maneuvers where the obstructed shoulder is rotated until the neonate faces toward the posterior of the mother [12,13]. Utilizing the oblique diameter offers approximately 2 cm of additional space for the neonatal shoulders [32]. Finally, for simulating the posterior arm delivery maneuver, the posterior arm of the neonate model was positioned extending out of the birth canal at the start of the simulation (Fig. 6).

During each simulation, the maternal endogenous force applied to the neonate's upper torso was incremented by 5N until delivery was achieved, starting from 0N. Delivery was defined as when the neonate's anterior shoulder cleared the maternal symphysis pubis, indicating alleviation of the obstruction, which was visually identified in MADPost, the software's postprocessor (Fig. 7) [26]. For each simulated condition, the minimum delivery force and the maximum BP strain, defined as BP strain in this study, was recorded. BP strain was calculated as the percent change in length of the BP (Δl) relative to the initial length of the BP, l_i, (i.e., 7.5 cm) as shown in Eq. (1) [26]

$$\text{BP strain}\,\% = \frac{\Delta l}{l_i} \times 100 \tag{1}$$

The sensitivity analysis was performed to understand the effects of variations in BP stiffness on the resulting BP strain. BP stiffness was changed by $\pm 10\%$ in the lithotomy alone position (without any additional neonate maneuvers), and the minimum delivery force and the maximum BP strain were recorded. Based on data from neonatal piglet BP studies [20], the range of stiffness values did not vary more than 10% of the average stiffness value for the MSC used in the current model.

Results

MADYMO models of a neonate and maternal pelvis were used to simulate the lithotomy position, application of SPPs (40N, 80N, or 140N), oblique position, and posterior arm delivery maneuvers. In each simulation, the maternal delivery force was measured as the minimum force required to achieve delivery. Delivery was confirmed when the obstruction of the neonatal anterior shoulder behind the maternal pelvis was alleviated. At the time of alleviation, the resulting BP strain was also measured. Starting with 0N of delivery force applied to the torso of the neonate, simulating no maternal expulsive forces through uterine contractions or Valsalva, the force was incremented by 5N until delivery of the neonate's anterior shoulder was observed. Required delivery forces and the resulting BP strain observed during various simulations are shown in Table 1.

The force required for delivery and resulting BP strain was dependent on the simulated maneuver. The lithotomy alone position

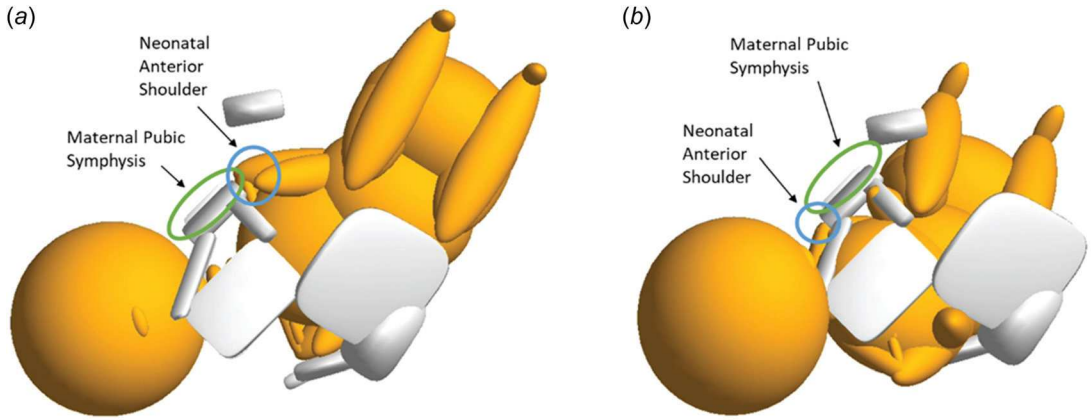

Fig. 7 The models at the beginning (*a*) and end of the simulation when delivery of the neonatal anterior shoulder is achieved (*b*)

Table 1 Required maternal delivery force and resulting brachial plexus strain for each maneuver simulation applied in the lithotomy position and its comparison to previously reported study [26]

	Current study			2010 study [26]		
Maneuver/position	Required delivery force (N)	Resulting BP strain (%)	Reduction in BP strain from lithotomy position (%)	Required delivery force (N)	Resulting BP strain (%)	Reduction in BP strain from lithotomy position (%)
Lithotomy	140	19.22	—	75	13.5	—
SPP 40N	120	16.36	14.88	65	11.5	14.8
SPP 80N	80	16.27	15.35	55	10.8	20
SPP 140N	75	15.71	18.26	45	10.4	23
Oblique	30	11.11	42.20	40	10.5	22.2
Posterior arm delivery	5	8.39	56.35	15	3.9	71.1

Table 2 Sensitivity analysis investigating the effects of varying BP stiffness (+/−10%) on BP strain during lithotomy alone position

BP stiffness (N/m)	Required delivery force (N)	Resulting BP strain (%)
240.46 (−10%)	140	19.480
267.18	140	19.220
293.90 (+10%)	140	18.911

was treated as the baseline position and required 140N of maternal force to deliver the anterior shoulder with a neonatal BP strain of 19.22%, as shown in Table 1. Each of the successive maneuvers reported a decrease in both the required delivery force and resulting neonatal BP strain. The three independent simulations of different magnitudes of SPP forces (40N, 80N, or 140N) reported that as the applied SPP force increased, the required maternal delivery force and neonatal BP strain decreased. A reduction in both delivery force and neonatal BP strain was also observed in the oblique position, with a further decrease in the delivery force and neonatal BP strain during the posterior arm delivery maneuver.

The percentage reductions in the neonatal BP strain during the maneuvers when compared to the lithotomy alone are also summarized in Table 1. SPP forces of 40N, 80N, or 140N resulted in 14.88%, 15.35%, and 18.26% reduction in the BP strain, respectively, when compared to the lithotomy position. The oblique position led to a further reduction of 42.20% in BP strain, when compared to the lithotomy position. The lowest BP strain was observed during posterior arm delivery with a 56.35% reduction in BP strain when compared to the lithotomy position. The required delivery force also followed a similar trend.

The results of the sensitivity analysis investigating the effects of varying BP stiffness on BP strain during lithotomy alone position are shown in Table 2. The lithotomy position was simulated without any additional neonate maneuvers. The stiffness of the modeled BP was increased and decreased by 10% to demonstrate how sensitive the models were to the BP biomechanical properties.

Discussion

When shoulder dystocia occurs, it is essential that it be managed quickly, and carefully before serious injuries can occur to the mother or the neonate. Investigational clinical studies that can improve the clinical management of shoulder dystocia are not feasible due to ethical limitations and technical challenges within the clinical environment. Computational models like MADYMO serve as promising surrogates in providing predictive information about BP strain while simulating delivery maneuvers that are utilized during complicated delivery scenarios [20,26]. This study aimed to develop highly biofidelic MADYMO models of the neonate and maternal pelvis by making significant improvements to previously developed MADYMO models including the resizing and reorientation of the neonate model [23,26,29,30]. The model improvements included the sizing and orientation of the neonate model, anatomical location of the neonatal BP, force–displacement properties of the neonatal BP that were obtained from neonatal piglet MSC BP nerve, and the method of applying gravity to the models.

Furthermore, the study also aimed to report the BP strain responses in an array of widely utilized clinical maneuver simulations that are commonly employed and widely reported in the management of shoulder dystocia. The sequential neonate-focused maneuvers simulated independently in this study are clinically relevant and have been developed, practiced, and traditionally taught for the management of shoulder dystocia [3]. The simulated maneuvers demonstrated a trend between clinically applied delivery maneuvers and the minimum required delivery force and resulting neonatal BP strain. The lithotomy alone position resulted in the largest force required to deliver the neonate's anterior shoulder and the greatest amount of neonatal BP strain. This relationship between the applied maternal force and BP strain is expected, as there is advancement of the spine-neck-head complex, while the shoulder is restrained behind the maternal pelvis (Fig. 7). When 40N of SPP was applied, the required delivery force decreased, and neonatal BP strain was reduced by about 15% compared to the lithotomy alone simulation. The reduction was due to the downward force directly applied over the obstructed neonatal shoulder that moved the shoulder toward the maternal spine and under the symphysis pubis bone, thus alleviating the obstruction [18,33]. A further reduction in both required delivery force and neonatal BP strain was observed as the SPP force was applied. Furthermore, an increase in SPP force applied above the shoulder resulted in less interaction between the shoulder and the symphysis pubis, causing the contact force-driven neonatal BP strain to decrease [29,30]. The result of this simulation is shown in Fig. 8,

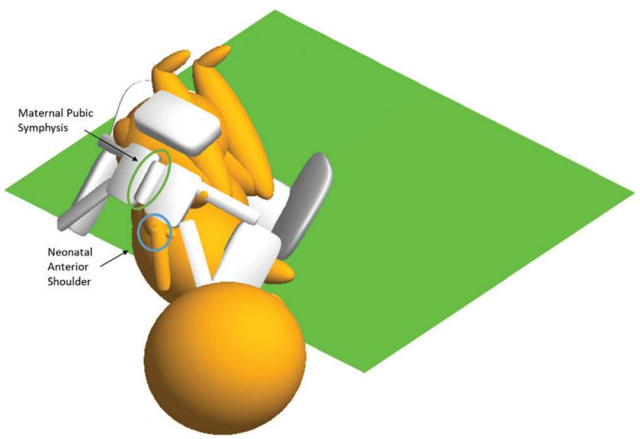

Fig. 8 Delivery simulation of 140N of suprapubic pressure (SPP) force applied above the neonatal shoulder

where a noticeable downward trajectory is observed due to the downward force applied by the clinician. A reduction in the required delivery force was also observed as the applied SPP force increased.

In clinical scenarios, the oblique position of the infant can be achieved when the clinician applies pressure to the anterior aspect of the posterior shoulder (Wood's screw) or the posterior aspect of the anterior shoulder (Rubin II maneuver) to rotate the neonate in a corkscrew-like motion by about 30 deg [3,12,34]. For this study, a similar simulation was performed, where the neonatal model was rotated 30 deg clockwise – moving the anterior shoulder toward the posterior aspect of the maternal pelvis. In the current study, the rotational maneuvers, modeled by the oblique positioning, reported a further reduction in the required delivery force and neonatal BP strain when compared to the application of SPP forces (32% reduction from SPP of 40N, 29% reduction from SPP of 140N) and lithotomy alone (42% reduction) simulations. The observed reduction in the oblique position can be attributed to the alignment of the neonate's shoulder width, or the bisacromial diameter, with the maternal pelvis' oblique diameter [21]. The oblique diameter of the maternal pelvis is the largest measurement of the diagonal space between the left and right halves of the pelvis and is larger than the obstetric conjugate, which is the smallest of the diameters of the pelvis. In the simulations of the maneuvers in this study, except for the oblique position, the bisacromial diameter of the neonate model aligned with the obstetric conjugate of the pelvis model [1,6].

The posterior arm delivery maneuver simulation, in this study, resulted in the smallest amount of required delivery force and neonatal BP strain. This was due to the reduction in the effective shoulder width after delivery of the posterior arm. Although this maneuver is the most invasive clinically and has an increased risk of neonatal humerus fracture, it effectively reduces the shoulder width by about 2 cm that helps achieve delivery [13].

The trends in the required delivery force and BP strain reported during various simulated maneuvers were similar between the current study and Grimm et al. [26], which looked at the effect of the maneuvers when clinician-applied, axial traction delivered the infant. Both studies demonstrated a decrease in BP strain as the magnitude of the SPP force increased [26]. The oblique maneuver resulted in the second greatest reduction in BP strain with 22.2% (maternal forces) and 42.2% (clinician-applied forces), in both the previous studies as well as the current study, respectively, when compared to delivery in the lithotomy alone position [26]. Finally, the posterior arm delivery maneuver also resulted in the greatest reduction in BP strain in both studies. Grimm et al. reported a 71.1% decrease in BP strain with posterior arm delivery when compared to the delivery facilitated by clinician-applied, axial traction in lithotomy position [26]. The current study also resulted in a 56.3% decrease in BP strain when maternal forces deliver the infant in the posterior arm position. The findings of the current study are also consistent with literature findings that report oblique and posterior arm delivery maneuvers to be effective in managing shoulder dystocia [17].

There are some limitations of the current study that are attributed to all computational modeling approaches. Clinically, there is high variability among cases including variability in anatomy, geometry, size, and shoulder dystocia occurrence, which cannot be captured in the computational models. Another limitation is the independently modeled simulations, while it has been reported that the risk of neonatal BP injury increases as the number of maneuvers performed successively increases [17]. The current study is limited in its approach and does not include the results of multiple sequential maneuvers.

Despite its limitations, the improved models used in this study offer useful insights into the effects of currently employed clinical maneuvers that help manage shoulder dystocia during complicated deliveries. Future studies can continue to utilize these models and investigate additional maneuvers, including the McRoberts maneuver, which is also commonly used during shoulder dystocia events. The McRoberts maneuver considers the orientation of the maternal pelvis and is therefore not a neonate-focused maneuver but should be included in future modeling studies. The combination of oblique positioning and SPP may also be simulated as literature has reported a further reduction of BP strain when applied in conjunction [12,13,35]. Studies can also focus on further enhancing the neonatal model by including in vivo BP biomechanical properties of a neonatal large animal model, thereby allowing the MADYMO model to more closely replicate the human BP responses. The utilized BP data reported in the Singh et al. study reported the in vitro BP properties [26]. In vivo BP failure data are currently unavailable and may vary from in vitro responses due to differences in loading and boundary conditions between in vivo and in vitro environments. Furthermore, future studies can correlate the obtained BP strain data with functional and structural injury thresholds, thereby enhancing the models' injury prediction abilities [36–38]. These developed computational models can serve as clinical investigational as well as educational tools that guide the development and training of delivery maneuvers that are effective in managing shoulder dystocia [39–41]. Alternative modeling approaches including Finite element (FE) modeling can also be beneficial in creating more robust neonate and maternal pelvis models that include soft tissue structures that play an important role in delivery mechanics and resulting BP strains [22,42]. The MADYMO modeling software is limited in its ability to define soft tissue properties which would more effectively be defined using FE modeling. These FE models can also incorporate patient-specific morphology as previous models were developed for pediatric scoliosis [43–46].

Acknowledgment

The authors would like to thank Marc Mounzer and Dr. Sheng Chen for their assistance with this project.

Funding Data

- Eunice Kennedy Shriver of National Institute of Child Health and Human Development of the National Institutes of Health (Award No. R15HD093024 R01HD104910A; Funder ID: 10.13039/100009633).
- National Science Foundation (Award No. 1752513; Funder ID: 10.13039/100000001).

Data Availability Statement

The datasets generated and supporting the findings of this article are obtainable from the corresponding author upon reasonable request.

References

[1] Menticoglou, S., 2018, "Shoulder Dystocia: Incidence, Mechanisms, and Management Strategies," Int. J. Womens Health, **10**, pp. 723–732.

[2] Ouzounian, J. G., 2016, "Shoulder Dystocia: Incidence and Risk Factors," Clin. Obstet. Gynecol., **59**(4), pp. 791–794.

[3] Williams, J. W., Cunningham, F. G., Leveno, K. J., Bloom, S. L., Spong, C. Y., and Dashe, J. S., 2018, *Williams Obstetrics*, 25th ed., McGraw-Hill Education Medical, New York.

[4] Gherman, R. B., Chauhan, S., Ouzounian, J. G., Lerner, H., Gonik, B., and Goodwin, T. M., 2006, "Shoulder Dystocia: The Unpreventable Obstetric Emergency With Empiric Management Guidelines," Am. J. Obstet. Gynecol., **195**(3), pp. 657–672.

[5] MacKenzie, I. Z., Shah, M., Lean, K., Dutton, S., Newdick, H., and Tucker, D. E., 2007, "Management of Shoulder Dystocia: Trends in Incidence and Maternal and Neonatal Morbidity," Obstet. Gynecol., **110**(5), pp. 1059–1068.

[6] Dunbar, D. C., Vilensky, J. A., Suarez-Quian, C. A., Shen, P. Y., Metaizeau, J. P., and Supakul, N., 2021, "Risk Factors for Neonatal Brachial Plexus Palsy Attributed to Anatomy, Physiology, and Evolution," Clin. Anat., **34**(6), pp. 884–898.

[7] Heinonen, K., Saisto, T., Gissler, M., Kaijomaa, M., and Sarvilinna, N., 2021, "Rising Trends in the Incidence of Shoulder Dystocia and Development of a Novel Shoulder Dystocia Risk Score Tool: A Nationwide Population-Based Study of 800 484 Finnish Deliveries," Acta Obstet. Gynecol. Scand., **100**(3), pp. 538–547.

[8] Orozco, V., Magee, R., Balasubramanian, S., and Singh, A., 2021, "A Systematic Review of the Tensile Biomechanical Properties of the Neonatal Brachial Plexus," ASME J. Biomech. Eng., **143**(11), p. 110802.

[9] Chauhan, S. P., Blackwell, S. B., and Ananth, C. V., 2014, "Neonatal Brachial Plexus Palsy: Incidence, Prevalence, and Temporal Trends," Semin. Perinatol., **38**(4), pp. 210–218.

[10] Sandmire, H. F., and DeMott, R. K., 2002, "Erb's Palsy Without Shoulder Dystocia," Int. J. Gynaecol. Obstet., **78**(3), pp. 253–256.
[11] Yang, L. J., 2014, "Neonatal Brachial Plexus Palsy–Management and Prognostic Factors," Semin. Perinatol., **38**(4), pp. 222–234.
[12] Gurewitsch, E. D., and Allen, R. H., 2005, "Fetal Manipulation for Management of Shoulder Dystocia," Fetal Maternal Med. Rev., **17**(3), pp. 239–280.
[13] Allen, R. H., 2007, "On the Mechanical Aspects of Shoulder Dystocia and Birth Injury," Clin. Obstet. Gynecol., **50**(3), pp. 607–623.
[14] Grimm, M. J., 2021, "Forces Involved With Labor and Delivery-A Biomechanical Perspective," Ann. Biomed. Eng., **49**(8), pp. 1819–1835.
[15] Nocon, J. J., McKenzie, D. K., Thomas, L. J., and Hansell, R. S., 1993, "Shoulder Dystocia: An Analysis of Risks and Obstetric Maneuvers," Am. J. Obstet. Gynecol., **168**(6), pp. 1732–1739.
[16] Gherman, R. B., Goodwin, T. M., Souter, I., Neumann, K., Ouzounian, J. G., and Paul, R. H., 1997, "The McRoberts' Maneuver for the Alleviation of Shoulder Dystocia: How Successful is It?," Am. J. Obstet. Gynecol., **176**(3), pp. 656–661.
[17] McFarland, M. B., Langer, O., Piper, J. M., and Berkus, M. D., 1996, "Perinatal Outcome and the Type and Number of Maneuvers in Shoulder Dystocia," Int. J. Gynaecol. Obstet., **55**(3), pp. 219–224.
[18] Lok, Z. L., Cheng, Y. K., and Leung, T. Y., 2016, "Predictive Factors for the Success of McRoberts' Manoeuvre and Suprapubic Pressure in Relieving Shoulder Dystocia: A Cross-Sectional Study," BMC Pregnancy Childbirth, **16**(1), p. 334.
[19] Leung, T. Y., Stuart, O., Suen, S. S., Sahota, D. S., Lau, T. K., and Lao, T. T., 2011, "Comparison of Perinatal Outcomes of Shoulder Dystocia Alleviated by Different Type and Sequence of Manoeuvres: A Retrospective Review," BJOG, **118**(8), pp. 985–990.
[20] Singh, A., Shaji, S., Delivoria-Papadopoulos, M., and Balasubramanian, S., 2018, "Biomechanical Responses of Neonatal Brachial Plexus to Mechanical Stretch," J. Brachial Plex Peripher. Nerve INJ., **13**(01), pp. e8–e14.
[21] DeSilva, J. M., Laudicina, N. M., Rosenberg, K. R., and Trevathan, W. R., 2017, "Neonatal Shoulder Width Suggests a Semirotational, Oblique Birth Mechanism in *Australopithecus Afarensis*," Anat. Rec. (Hoboken), **300**(5), pp. 890–899.
[22] Peters, J. R., Campbell, R. M., Jr., and Balasubramanian, S., 2017, "Characterization of the Age-Dependent Shape of the Pediatric Thoracic Spine and Vertebrae Using Generalized Procrustes Analysis," J. Biomech., **63**, pp. 32–40.
[23] Zhang, N., Gonik, B., and Grimm, M. J., 2003, "Development of a MADYMO Model to Investigate Fetal Brachial Plexus Injury During Complicated Vagial Delivery," Summer Bioengineering Conference, Key Biscayne, FL, June 25–29.
[24] Centers for Disease Control and Prevention, 2022, "Data Table of Infant Head Circumference-for-Age Charts," Centers for Disease Control and Prevention, National Center for Health Statistics, Atlanta, GA, accessed May 14, 2022, https://www.cdc.gov/growthcharts/html_charts/hcageinf.htm
[25] Verspyck, E., Goffinet, F., Hellot, M. F., Milliez, J., and Marpeau, L., 1999, "Newborn Shoulder Width: A Prospective Study of 2222 Consecutive Measurements," Br. J. Obstet. Gynaecol., **106**(6), pp. 589–593.
[26] Grimm, M. J., Costello, R. E., and Gonik, B., 2010, "Effect of Clinician-Applied Maneuvers on Brachial Plexus Stretch During a Shoulder Dystocia Event: Investigation Using a Computer Simulation Model," Am. J. Obstet. Gynecol., **203**(4), p. 339.
[27] Leinberry, C. F., and Wehbé, M. A., 2004, "Brachial Plexus Anatomy," Hand Clin., **20**(1), pp. 1–5.
[28] Rydevik, B. L., Kwan, M. K., Myers, R. R., Brown, R. A., Triggs, K. J., Woo, S. L., and Garfin, S. R., 1990, "An In Vitro Mechanical and Histological Study of Acute Stretching on Rabbit Tibial Nerve," J. Orthop. Res., **8**(5), pp. 694–701.
[29] Gonik, B., Zhang, N., and Grimm, M. J., 2003, "Prediction of Brachial Plexus Stretching During Shoulder Dystocia Using a Computer Simulation Model," Am. J. Obstet. Gynecol., **189**(4), pp. 1168–1172.
[30] Gonik, B., Zhang, N., and Grimm, M. J., 2003, "Defining Forces That Are Associated With Shoulder Dystocia: The Use of a Mathematic Dynamic Computer Model," Am. J. Obstet. Gynecol., **188**(4), pp. 1068–1072.
[31] Siemens, 2017, "MADYMO Theory Manual," *Design, Simulation and Virtual Testing*, Siemens, Portland, OR.
[32] Gherman, R. B., Ouzounian, J. G., and Goodwin, T. M., 1998, "Obstetric Maneuvers for Shoulder Dystocia and Associated Fetal Morbidity," Am. J. Obstet. Gynecol., **178**(6), pp. 1126–1130.
[33] Penney, D. S., and Perlis, D. W., 1992, "Shoulder Dystocia: When to Use Suprapubic or Fundal Pressure," MCN Am. J. Matern. Child Nurs., **17**(1), pp. 34–36.
[34] Mazzanti, G. A., 1959, "Delivery of the Anterior Shoulder; a Neglected Art," Obstet. Gynecol., **13**(5), pp. 603–607.
[35] Hoffman, M. K., Bailit, J. L., Branch, D. W., Burkman, R. T., Van Veldhusien, P., Lu, L., et al. 2011, "A Comparison of Obstetric Maneuvers for the Acute Management of Shoulder Dystocia," Obstet. Gynecol., **117**(6), pp. 1272–1278.
[36] Singh, A., 2017, "Extent of Impaired Axoplasmic Transport and Neurofilament Compaction in Traumatically Injured Axon at Various Strains and Strain Rates," Brain INJ, **31**(10), pp. 1387–1395.
[37] Singh, A., Magee, R., and Balasubramanian, S., 2019, "Methods for In Vivo Biomechanical Testing on Brachial Plexus in Neonatal Piglets," J. Vis. Exp., (154).
[38] Singh, A., Kallakuri, S., Chen, C., and Cavanaugh, J. M., 2009, "Structural and Functional Changes in Nerve Roots Due to Tension at Various Strains and Strain Rates: An in-Vivo Study," J. Neurotrauma, **26**(4), pp. 627–640.
[39] Singh, A., Ferry, D., and Balasubramanian, S., 2019, "Efficacy of Clinical Simulation-Based Training in Biomedical Engineering Education," ASME J. Biomech. Eng., **141**(12), p. 121011.
[40] Singh, A., 2017, "A New Approach to Teaching Biomechanics Through Active, Adaptive, and Experiential Learning," ASME J. Biomech. Eng., **139**(7), p. 071001.
[41] Singh, A., Ferry, D., Ramakrishnan, A., and Balasubramanian, S., 2020, "Using Virtual Reality in Biomedical Engineering Education," ASME J. Biomech. Eng., **142**(11), p. 111013.
[42] Balasubramanian, S., D'Andrea, C. R., Viraraghavan, G., and Cahill, P. J., 2022, "Development of a Finite Element Model of the Pediatric Thoracic and Lumbar Spine, Ribcage, and Pelvis With Orthotropic Region-Specific Vertebral Growth," ASME J. Biomech. Eng., **144**(10), p. 101007.
[43] Balasubramanian, S., Peters, J. R., Robinson, L. F., Singh, A., and Kent, R. W., 2016, "Thoracic Spine Morphology of a Pseudo-Biped Animal Model (Kangaroo) and Comparisons With Human and Quadruped Animals," Eur. Spine J., **25**(12), pp. 4140–4154.
[44] Peters, J. R., Chandrasekaran, C., Robinson, L. F., Servaes, S. E., Campbell, R. M., Jr., and Balasubramanian, S., 2015, "Age-and Gender-Related Changes in Pediatric Thoracic Vertebral Morphology," Spine J., **15**(5), pp. 1000–1020.
[45] Hadagali, P., Peters, J. R., and Balasubramanian, S., 2018, "Morphing the Feature-Based Multi-Blocks of Normative/Healthy Vertebral Geometries to Scoliosis Vertebral Geometries: Development of Personalized Finite Element Models," Comput. Methods Biomech. Biomed. Eng., **21**(4), pp. 297–324.
[46] Peters, J. R., Servaes, S. E., Cahill, P. J., and Balasubramanian, S., 2021, "Morphology and Growth of the Pediatric Lumbar Vertebrae," Spine J., **21**(4), pp. 682–697.